HHS Public Access

Author manuscript

ACS Nano. Author manuscript; available in PMC 2023 May 19.

Published in final edited form as:

ACS Nano. 2023 February 28; 17(4): 3966–3975. doi:10.1021/acsnano.2c12754.

Bioinspired CRISPR-Mediated Cascade Reaction Biosensor for Molecular Detection of HIV Using a Glucose Meter

Ziyue Li[1,2], **Naoki Uno**[1], **Xiong Ding**[1], **Lori Avery**[3], **David Banach**[4], **Changchun Liu**[1,*]

[1]Department of Biomedical Engineering, University of Connecticut Health Center, Farmington, CT 06030, United States

[2]Department of Biomedical Engineering, University of Connecticut, Storrs, CT 06269, United States

[3]Department of Pathology and Laboratory Medicine, University of Connecticut Health Center, Farmington, CT 06030, United States

[4]Department of Medicine, Division of Infectious Diseases, University of Connecticut Health Center, Farmington, CT 06030, United States

Abstract

HIV molecular detection plays a significant role in early diagnosis and antiretroviral therapy for HIV patients. CRISPR technology has recently emerged as a powerful tool for highly sensitive and specific nucleic acid-based molecular detection when used in combination with isothermal amplification. However, it remains a challenge to improve the compatibility of such a multi-enzyme reaction system for simple and sensitive molecular detection. Inspired by the multi-compartment structures in a living cell, we present a nanoporous membrane-separated (compartmentalized), artificial, cascade reaction system to improve the compatibility of a CRISPR-mediated multi-enzyme reaction. We further integrated the multi-enzyme cascade reaction system with a microfluidic platform and glucose biosensing technology to develop a bioinspired, CRISPR-mediated cascade reaction (CRISPR-MCR) biosensor, enabling HIV molecular detection by a simple glucose meter, analogous to diabetes home testing. We applied

[*]**Corresponding author**: Dr. Changchun Liu, Department of Biomedical Engineering, University of Connecticut Health Center, 263 Farmington Avenue, Farmington, CT 06030, Phone: (860)-679-2565, chaliu@uchc.edu.

Author Contributions

Z.L. and C.L. conceived the idea. Z.L., N.U., X.D. and L.A. carried out the experiments. Z.L., N.U., X.D., D.B. and C.L. analyzed the data. C.L. supervised the project. Z.L. and C.L. wrote the manuscript. All authors discussed the results and commented on the manuscript.

The authors declare no competing financial interest.

Supporting Information

The supporting information is available at

- Schematic illustration of the bioinspired CRISPR-MCR biosensor, exploded view and assembled view of the CRISPR-MCR biosensor, energy dispersive X-ray spectroscopy (EDS) of the MB-ssDNA-invertase reporter, quantitative detection of various HIV DNA plasmid target concentration by digital PCR chips, real-time fluorescence detection of CRISPR reaction after separate RPA preamplification of the various HIV DNA plasmid targets, representative fluorescence image of the digital PCR chip for HIV-1 RNA quantification, real-time fluorescence detection of CRISPR reaction after separate RT-RPA pre-amplification of the various HIV RNA targets, workflow of the bioinspired CRISPR-MCR biosensor for HIV detection, fluorescence image of the digital chips for HIV quantitative detection of sample S11 and S14, quantitative detection of different primary components in the CRISPR-MCR reaction system, summary of CRISPR-powered nucleic acid biosensors, and list of all oligonucleotide sequences used.

the bioinspired CRISPR-MCR biosensor to detect HIV DNA and HIV RNA, achieving a detection sensitivity of 43 copies and 200 copies per test, respectively. Further, we successfully validated the bioinspired biosensor by testing clinical plasma samples of HIV, demonstrating its great application potential for point-of-care testing of HIV virus and other pathogens at home or in resource-limited settings.

Graphical Abstract

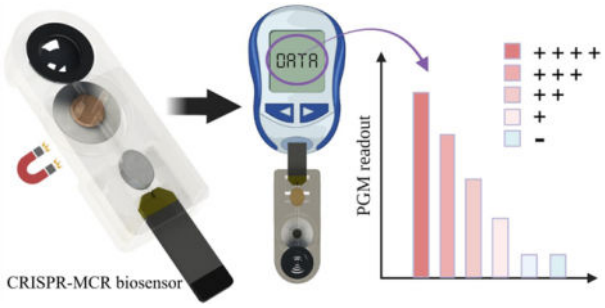

Keywords

CRISPR-based nucleic acid detection; nanoporous membrane; electrochemical biosensor; microfluidic technology; HIV molecular detection

HIV virus, which causes acquired immunodeficiency syndrome (AIDS), is one of the world's most serious public health challenges[1]. Simple, sensitive, and affordable molecular detection of HIV plays a crucial role in the early diagnosis, timely treatment, and antiretroviral therapy (ART) of HIV patients[1–3]. Quantitative reverse transcription-polymerase chain reaction (RT-qPCR), which is considered the gold standard of HIV virus testing, typically requires expensive instruments and highly trained personnel, all of which limit its utilization to only well-equipped laboratories. Therefore, there is an unmet need for a rapid, sensitive and affordable approach for molecular detection of HIV at the point of care.

In recent years, clustered regularly interspaced short palindromic repeats (CRISPR)-associated (Cas) proteins (e.g., Cas12a and Cas13a) have emerged as powerful point of care tools for nucleic acid-based molecular detection of different pathogens[4–9] For instance, researchers have combined CRISPR detection with isothermal amplification technologies, including recombinase polymerase amplification (RPA) and loop-mediated isothermal amplification (LAMP), to develop sensitive and specific CRISPR-based molecular diagnostic technologies, such as SHERLOCK (Specific High-sensitivity Enzymatic Reporter UnLOCKing)[4,5] and DETECTR (DNA Endonuclease-Targeted CRISPR Trans Reporter)[6,7]. However, the isothermal amplification reaction and CRISPR detection systems have limited compatibility due to the different enzymes and reaction buffer components. Thus, these methods typically require separate reaction tubes and involve multiple manual operations (e.g., transferring amplification products), which potentially increases the carry-over contamination risk and is not ideal for point-of-care applications.

In living cells (e.g., eukaryotic cells), different enzymes spatially defined within subcellular organelles work together in multi-step (sequential) reactions like a cascade system[10–13], where the reaction product generated by the first enzyme serves as the substrate for the next one (Figure 1A). Due to spatially confined enzymatic reactions, a membrane-separated, compartmentalized reaction system provides a simple and straightforward strategy to achieve high compatibility of multi-enzyme biochemical reactions, which often have different reaction conditions (e.g., buffer components, enzymes, ion concentrations) or show mutual inhibition. Recently, considerable efforts have focused on creating artificial multi-enzyme cascade reaction systems for various biochemical applications, such as chemical synthesis[14,15], disease therapy[16], and biological detoxification[17]. Despite significant progress, nucleic acid detection in a compartmentalized cascade reaction system has rarely been explored and remains challenging[18].

In this study, inspired by the multi-compartment structures in a living cell, we propose a nanoporous membrane-separated (compartmentalized), artificial, cascade reaction system to improve the compatibility of CRISPR-mediated multi-enzyme reactions. To adapt the cascade reaction system to a simple point-of-care molecular diagnostic application, we further integrated the compartmentalized cascade reaction system with a microfluidic platform and glucose biosensing technology to develop a bioinspired, CRISPR-mediated cascade reaction (CRISPR-MCR) biosensor for HIV molecular detection. The HIV nucleic acid can be digitally detected through a personal glucose meter at the endpoint, analogous to reading glucose levels in blood, eliminating the need for an expensive instrument (e.g., PCR thermocycler). We used the bioinspired CRISPR-MCR biosensor to detect both HIV DNA plasmid and HIV viral RNA. To demonstrate its clinical utility, we further utilized the bioinspired CRISPR-MCR biosensor to detect HIV virus in clinical plasma samples.

RESULTS AND DISCUSSION

Principle and Construction of the Bioinspired CRISPR-MCR Biosensor.

To improve the compatibility of a multi-enzyme reaction system (e.g., CRISPR-Cas12a, DNA polymerase), we developed a nanoporous membrane-separated, artificial, cascade reaction system inspired by the elegant multi-compartment structures of the living cell (Figure 1A and B). In the CRISPR-mediated cascade reaction system, the porous membrane separates the reaction system into two reaction chambers: i) a lower RPA/RT-RPA reaction chamber, and ii) an upper CRISPR reaction chamber. As shown in Figure 1B, the two reaction chambers are spatially separated but connected through a nanoporous membrane (right bottom inset). In the presence of HIV nucleic acid, millions of RPA amplicons are generated in the RPA reaction chamber due to exponential amplification of the DNA. These short amplicons (137 bp) can easily diffuse into the CRISPR reaction chamber through the nanoporous membrane due to the concentration gradient (difference) and small molecule size, which leads to specific activation of the CRISPR-Cas12a enzyme in the CRISPR reaction chamber. Thus, the activated CRISPR-Cas12a non-specifically cuts the single-stranded DNA (ssDNA)-conjugated invertase immobilized on the magnetic beads, resulting in the release of free invertase for downstream electrochemical detection. On the contrary, the rapid diffusion of other biological molecules, including enzymes and potential

inhibitors, are limited or delayed by the nanoporous membrane between the two reaction chambers, which significantly improves the compatibility of the CRISPR cleavage reaction and electrochemical detection.

To adapt the CRISPR-mediated cascade reaction system for point-of-care diagnostic applications, we further integrated it into a microfluidic platform and with glucose electrochemical biosensing technology to develop a bioinspired CRISPR-MCR biosensor for molecular detection of HIV by using a personal glucose meter (Figure 1C, Supplementary Figure S1 and S2). The bioinspired biosensor contains four major functional units: i) a blister pouch filled with water, ii) a membrane-separated, CRISPR-mediated cascade reaction system, iii) an invertase-catalyzed glucose chamber with pre-stored, lyophilized, sucrose substrate, which can be hydrolyzed into glucose in the presence of the invertase enzyme, and iv) a glucose testing strip for electrochemical biosensing detection (Figure 1C). To enable simple electrochemical detection of HIV nucleic acid by the glucose meter (Figure 1D), we used magnetic beads immobilized with ssDNA-invertase (termed "MB-ssDNA-invertase") conjugates as the reporter of our biosensor (Figure 1B). In the presence of the HIV nucleic acid, the CRISPR enzyme will be activated to cleave the ssDNA of the MB-ssDNA-invertase, resulting in the release of the free invertase enzyme in the CRISPR reaction chamber. When the blister is pressed, the pre-stored water moves the free invertase released from the magnetic beads into the invertase-catalyzed glucose chamber while the magnetic beads remain in the CRISPR reaction chamber due to the magnetic force generated by the neodymium disc magnet under the biosensor. In the catalytic chamber, the invertase enzyme hydrolyzes pre-stored sucrose into the glucose, which can be detected by the glucose meter (left inset, Figure 1C). Thus, the HIV nucleic acid can be digitally detected by a personal glucose meter (Figure 1D), analogous to home diabetes testing and eliminating the need for complex equipment (e.g., PCR thermal cycler).

Nanoporous Membrane-separated, Artificial, CRISPR-mediated Cascade Reaction System.

To simplify the testing operation and minimize the carry-over contamination, researchers have proposed several strategies to combine nucleic acid amplification and the CRISPR reaction process into a single "one-pot" reaction system, such as the physical separation method[19,20], multi-phase reaction[18,21] and engineered CRISPR crRNA[22,23]. In our initial experiment, we tried to adapt a "one-pot" approach without membrane separation to develop our CRISPR-based nucleic acid detection by using a glucose meter. Unfortunately, we found that the RPA reaction solution significantly interferes with the CRISPR reaction and electrochemical detection, even resulting in false negative signals (Figure 2A). Interestingly, the higher the volume of the RPA reaction solution, the lower the electrochemical detection signal in the same detection sample (Figure 2A). In particular, the personal glucose meter readout drops to 10 mg/dL or below when the volume of the RPA reaction solution is at or above 64% of the whole reaction volume (total volume 25 μL). Therefore, we decided to use a porous membrane to separate the RPA reaction solution from the other reaction solution and minimize its interference effect to the CRISPR-mediated cascade reaction.

To optimize the compartmentalized, CRISPR-mediated cascade reaction system, we first tested and compared the performance of different hydrophilic porous membranes with

a low protein binding property. To monitor the CRISPR reaction in real time, we introduced the single-stranded DNA fluorophore-quencher (ssDNA-FQ) reporter into the CRISPR reaction chamber and recorded the fluorescence intensity of the CRISPR reaction chamber by a portable USB fluorescence microscope. As shown in Figure 2B, both polyvinylidene fluoride (PVDF) membrane and polyethersulfone (PES) membrane worked well in our compartmentalized, CRISPR-mediated cascade reaction system. However, the PES membrane showed approximately two times higher fluorescence signal than the PVDF membrane in the CRISPR-mediated cascade reaction system. Thus, we selected the porous PES membrane to further develop our bioinspired CRISPR-MCR biosensor.

PES membranes have been widely used for biochemical separation applications because of their high hydrophilicity, excellent chemical resistance, and low protein binding properties[24,25]. To optimize the PES membrane for our system, we further determined the effect of the membrane pore size on the CRISPR-mediated cascade reaction. We evaluated and compared four commercially available PES membranes with various pore sizes ranging from 0.03 to 8 μm (Figure 2C and D). Surprisingly, the fluorescence signal of the CRISPR-mediated cascade reaction system significantly increased when the pore size of the PES membrane decreased (Figure 2C). For instance, the fluorescence intensity of the compartmentalized, cascade reaction system with an 0.03 μm porous membrane was two times stronger than that of the system with an 8 μm porous membrane. Although a larger pore size facilitates the rapid diffusion of DNA amplicon biomolecules, it enables and speeds up the diffusion of other molecules (e.g., enzymes) between the reaction chambers, reducing the enzymatic reaction efficiency and resulting in low fluorescence signal. To further validate it, we tested and compared the relative diffusion rate of several primary components in our CRISPR-MCR reaction system, including RT-RPA amplicons (dsDNA), RPA enzymes, Lba Cas12a enzyme and Invertase enzyme. As shown in Figure 2E, for all these molecules, the smaller the pore sizes of the PES membranes are, the lower their relative diffusion rate is. Especially, the diffusion of the enzymes was significantly limited by the 0.03 μm porous PES membrane because of the relatively large molecule size of these proteins. Thus, the 0.03 μm porous PES membrane could efficiently confine different functional enzymes in their own compartmentalized reaction chambers, enabling highly efficient CRISPR-MCR assay. Although the diffusion process of RT-RPA amplicons was also restricted, there are still sufficient DNA amplicons diffusing into the CRISPR reaction chamber due to: i) a high concentration gradient caused by the exponential amplification of the RPA reaction, and ii) the smaller molecular size of DNA amplicons (e.g., 137 bp) compared to proteins. Therefore, we applied the 0.03 μm nanoporous PES membrane in the bioinspired CRISPR-MCR biosensor for our subsequent experiments.

Electrochemical Detection of HIV Nucleic Acids by a Personal Glucose Meter.

We used three-dimensional (3D)-printing technology to fabricate our bioinspired CRISPR-MCR biosensor (Figure 3A and Supplementary Figure S2) because of its simplicity and low cost[26–28]. To adapt our biosensor to detect HIV nucleic acid by using a simple glucose meter, we used magnetic beads immobilized with ssDNA-invertase conjugates as the electrochemical detection reporter (Figure 3B). To functionalize the magnetic beads with the invertase conjugates, we first mixed the streptavidin magnetic beads with biotin-

ssDNA-invertase (BsI) conjugates and then washed the magnetic beads to remove the free conjugates according to previous literature[29,30]. To optimize the immobilization efficiency, we determined the ratio of the streptavidin magnetic beads and BsI conjugates by adding various amounts of the magnetic beads (from 0.2 to 1 mg) to 100 pmole BsI conjugates. After magnetic separation, we washed the synthesized MB-ssDNA-invertase reporter using washing buffer at least twice. Next, we introduced 40 μL of 50 mM sucrose solution and incubated the solution at 40°C for 10 min. We then detected the glucose generated from sucrose hydrolysis by the glucose meter. As shown in Figure 3B, the higher the usage amount of the magnetic beads, the higher the electrochemical signal of the glucose meter. When the usage amount was 0.8 mg or higher, the electrochemical readout of the glucose meter reached saturation. Thus, we used 0.8 mg magnetic beads per 100 pmole BsI probe to synthesize the MB-ssDNA-invertase reporter.

Next, we evaluated the usage of the MB-ssDNA-invertase reporter to optimize the CRISPR-mediated electrochemical detection. We tested different amounts of MB-ssDNA-invertase reporters (0.2, 0.4, 0.8, 1.6, and 2.4 mg) in a 50 μL CRISPR reaction system. After a 60-min incubation at 40°C, the magnetic beads were separated from the CRISPR reaction solution. Next, 20 μL supernatant containing released invertase was mixed with 20 μL 100 mM sucrose solution and incubated at 40°C for 10 min. Then, the generated glucose was quantified by the glucose meter. As shown in Figure 3C, the greater the amount of MB-ssDNA-invertase reporter, the higher the glucose meter's readout. However, using too much of the MB-ssDNA-invertase reporter significantly increases the testing cost. Thus, we used 2 mg MB-ssDNA-invertase reporter in the 50 μL reaction solution, which corresponds to a final concentration of 40 μg/μL in the CRISPR reaction system. To obtain direct information of the MB-ssDNA-invertase reporter, we investigated its morphology by SEM and transmission electron microscopy (TEM) (Figure 3D and 3E) and performed a surface analysis by energy dispersive X-ray spectroscopy (EDS) (Supplementary Figure S3). As shown in Figure 3E, the invertase layer can be clearly observed as a light-colored coating on the surface of the MB-ssDNA-invertase reporter.

Detection of HIV Nucleic Acid with the CRISPR-MCR Biosensors.

With the optimized experimental conditions above, we designed and developed a bioinspired CRISPR-MCR biosensor integrated with the CRISPR cascade reaction system and evaluated its analytical performance for detection of HIV nucleic acid. We determined the performance of the bioinspired CRISPR-MCR biosensor by testing HIV DNA plasmid and HIV RNA samples. We first detected HIV DNA plasmid in the bioinspired biosensor. We used digital PCR to quantify the HIV DNA plasmid samples (Supplementary Figure S4). As shown in Figure 4A, the longer the catalytic reaction time, the higher the electrochemical signal. At a fixed catalytic reaction time (e.g., five min), the biosensor could consistently detect 43 copies of HIV DNA plasmid per test, which is comparable to that of conventional fluorescence-based RPA/CRISPR detection (Supplementary Figure S5).

Next, we detected HIV RNA by using the bioinspired biosensor. We extracted the HIV RNA targets from commercially available HIV-positive controls. To enable accurate evaluation, we detected and quantified the HIV RNA by digital RT-PCR (Supplementary Figure

S6). As shown in Figure 4B, similar to the HIV DNA plasmid detection, the higher the HIV RNA target concentration, the stronger the electrochemical detection signal. In addition, with an increase in the catalytic reaction time, the background signal of the electrochemical detection increased, which may be attributed to the presence of unexpected free invertase molecules during the preparation of the MB-ssDNA-invertase reporter. Overall, the bioinspired biosensor can consistently detect HIV RNA with a sensitivity of 200 copies per test, which is comparable to the fluorescence-based RT-RPA/CRISPR detection using a real-time PCR machine (Supplementary Figure S7).

Clinical Validation of the Bioinspired CRISPR-MCR Biosensor for HIV Virus Detection.

To further validate the clinical utility of our bioinspired CRISPR-MCR biosensor, we detected HIV clinical samples, including HIV-positive and HIV-negative samples determined by standard RT-PCR (Figure 5A). To ensure reliable testing, we tested each sample three or four times. HIV RNA was first extracted from the clinical plasma samples by using commercial nucleic acid extraction kits. When testing for HIV by the bioinspired biosensor, the biosensor was first incubated in the heater at 40°C for 60 min for the RT-RPA/CRISPR reaction. After pressing the water blister, the device was incubated at 40°C for 10 min for the invertase catalysis. Then, the biosensing strip of the bioinspired biosensor was inserted into the glucose meter for HIV detection (Supplementary Figure S8). Figure 5B displays the representative HIV test results of 15 clinical samples and positive/negative controls on the bioinspired CRISPR-MCR biosensors by the glucose meter. When the readout of the glucose meter shows under-range (LO), it means that the glucose level is below 10 mg/dL. According to the 3 σ criterion[31,32], the cut-off threshold of 14 mg/dL is calculated and set as $\mu \pm 3\sigma$, where μ is the mean value of the negative control and σ is the standard deviation (sd).

Figure 5C shows the quantification cycle (Cq) values for clinical samples by the RT-qPCR method. Each sample was tested three times. All the data are presented as mean ±sd. When the cutoff (Cq = 39) was applied, seven samples were determined to be positive, and eight samples were negative. Sample S11 and S14 had an average Cq value of 38.7 and 39.6, respectively, in the RT-PCR method, both close to the cutoff Cq of 39. To further confirm these samples, we utilized the digital RT-PCR method. As shown in Supplementary Figure S9, sample S11 showed a weak positive signal in the digital RT-PCR chip. According to the quantitative result of the digital RT-PCR, the target concentration of sample S11 was estimated to be 170 copies per test in our biosensor detection, which is slightly below its detection sensitivity of 200 copies per test. For sample S14, we could not detect any positive signal in the digital RT-PCR chip, which is consistent with that of our bioinspired CRISPR-MCR biosensor. Therefore, as a simple, low-cost, portable molecular diagnostic device, our bioinspired CRISPR-MCR biosensor provides a promising diagnostic alternative to HIV virus detection and quantification.

CONCLUSIONS

In this study, we have presented an artificial, compartmentalized, cascade reaction system embedded with a nanoporous membrane, thus improving the compatibility of a CRISPR-

mediated, multi-enzyme reaction for nucleic acid detection. We further integrated the compartmentalized cascade reaction system into a microfluidic platform and developed a simple, portable bioinspired CRISPR-MCR biosensor for HIV nucleic acid quantification by using a low-cost glucose meter, eliminating the need for complex instruments and well-trained personnel. We applied our bioinspired CRISPR-MCR biosensor to detect HIV, achieving detection sensitivities of 43 copies of HIV DNA plasmid and 200 copies of HIV RNA per test, respectively. Further, we clinically validated the bioinspired biosensor by testing HIV virus in clinical plasma samples and obtained comparable performance with the state-of-the-art RT-PCR method. In the future, we will integrate the nucleic acid extraction function unit into the microfluidic biosensor to develop an integrated "sample-to-result" molecular detection device.[33] In addition, the detection time may be further reduced by using engineered CRISPR crRNAs.[34,35] Overall, our simple, sensitive bioinspired CRISPR-MCR biosensor exhibits great potential for rapid detection of HIV virus and other infectious diseases at the point of care.

MATERIALS AND METHODS

(RT)RPA/CRISPR reaction system.

The (RT)RPA/CRISPR reaction system was developed according to the literature.[6,28] The RPA kit, TwistAmp® Basic, was obtained from Twist Dx Limited (Maidenhead, UK). Rnase H and nuclease-free water were purchased from New England BioLabs (MA, USA). SuperScript™ IV Reverse Transcriptase was purchased from ThermoFisher Scientific (MA, USA). HIV plasmid and HIV primers (Supplementary Table S2) were synthesized from Integrated DNA Technologies (IA, USA). AcroMetrix™ HIV High Control and ACCURUN® 315 Series 500 HIV RNA Positive Control were purchased from ThermoFisher Scientific and SeraCare (MA, USA), respectively. The final 50 μL RT-RPA reaction system contained 1 dried pellet, 29.5 μL primer-free rehydration buffer, 0.5 μM each for forward and reverse HIV primers, 2 U/μL Superscript IV reverse transcriptase, 0.1 U/μL Rnase H, 14 mM MgOAc, and 1 μL target RNA extracted from an HIV-positive control. For the RPA reaction, reverse transcriptase was not included, and HIV DNA plasmid was tested.

Lba Cas12a was purchased from New England BioLabs (MA, USA). CRISPR RNA (crRNA) and fluorescent reporter (ssDNA-FQ) (Supplementary Table S2) were synthesized from Integrated DNA Technologies. The final volume of the CRISPR reaction was 50 μL, containing 400 nM Lba Cas12a, 200 nM each HIV crRNA1 and HIV crRNA2, 1X NEBuffer 2.1 (50 mM NaCl, 10 mM Tris-HCl, 10 mM $MgCl_2$, 100 μg/mL BSA, pH 7.9, 25 °C), RPA product, and reporter. For fluorescence detection, 4 μM fluorescent reporter ssDNA-FQ was used. For personal glucose meter detection in the bioinspired CRISPR-MCR biosensor, ssDNA-FQ was replaced with the MB-ssDNA-invertase reporter.

MB-ssDNA-invertase reporter synthesis.

Dynabeads™ M-280 Streptavidin was purchased from ThermoFisher Scientific. Oligo invertase conjugation BsI probe (Supplementary Table S2) was synthesized by Biosynthesis (TX, USA). Washing buffer (0.1 M NaCl, 0.1 M Na_3PO_4, pH 7.3, 25°C), preservation buffer

(0.1 M NaCl, 0.1 M Na_3PO_4, 0.05% Tween-20, pH 7.3, 25°C), and sucrose solution (50 mM and 100 mM, pH 7.3, 25°C) were prepared in the laboratory. To synthesize the MB-ssDNA-invertase reporter, the MB solution was first washed with washing buffer thoroughly and the supernatant was discarded. Typically, each 1 mg MB was washed with 80 μL washing buffer. Next, 100 pmole BsI probe was added to 0.8 mg MB in a 50 μL reaction solution and mixed at room temperature for 20 min. After thoroughly washing with the buffer to remove the free BsI probe, the MB-ssDNA-invertase reporter was ready for use. For future use, the preservation solution was used to store the MB-ssDNA-invertase reporter in a 4°C refrigerator. The preservation solution is discarded before use.

Real-time fluorescent detection in the CRISPR-MCR biosensor.

In real-time fluorescent detection of RPA/CRISPR reaction in the CRISPR-MCR biosensor, 50 μL RPA reaction solution with or without target template was inserted into the RPA/RT-RPA chamber, and 50 μL CRISPR reaction solution containing ssDNA-FQ reporter was introduced into the CRISPR chamber. Next, the biosensor was sealed by Microseal 'B' PCR Plate Sealing Film (Bio-Rad, CA, USA) and incubated on Mini Block Heater (VWR) at 40 °C. In the meanwhile, a portable USB fluorescence microscope (AM4113T-GFBW, Dino-Lite Premier, AnMo Electronics, Taiwan, China) was used to record the fluorescence signals in real time. Further, the fluorescence photos of the CRISPR reaction chamber were acquired and generated normalized average fluorescence intensities at every specified time interval (e.g., 1 min interval). Normalized fluorescence intensities were plotted against time to obtain real-time fluorescence curves.

Diffusion rate experiment.

RPA enzymes were acquired from TwistAmp® Liquid Basic RPA kit from Twist Dx Limited (Maidenhead, UK). Lba Cas12a enzyme was purchased from New England BioLabs (MA, USA). Invertase (CAS:9001–57-4) was purchased from Sigma-Aldrich (MO, USA). 137-bp dsDNA (Supplementary Table S2) was synthesized from Integrated DNA Technologies (IA, USA) as the RPA amplicons. The spectrophotometer analysis was performed by NanoDrop™ OneC Microvolume UV-Vis Spectrophotometer purchased from Thermo Fisher Scientific (MA, USA). Before carrying out the diffusion experiment, we determined and evaluated the detection sensitivity and quantitative range of the spectrophotometer by using a serial dilution of these components (Supplementary Figure S10). In the diffusion experiment, we separately prepared 10 μM dsDNA, 2* RPA enzymes mixture, 2 μM Lba Cas12a and 10 mg/mL Invertase as their own initial solution. To avoid mutual interference of different components during measurement, the diffusion experiment of each component was run independently. First, we introduced the initial solution into one chamber (termed "Initial chamber") of the CRISPR-MCR biosensor and water into another chamber (termed "Blank chamber"). Then, the biosensor was incubated in the mini-heater at 40°C for 1 hour like our CRISPR-MCR assay. Next, we collected the solution in the Blank chamber and measured the component's concentration. Theoretically, at the ideal diffusion equilibrium condition, the component will uniformly diffuse into the blank chamber and form a homogeneous solution in two chambers. Thus, the component's concentration in two chambers is the same and can be calculated based on its initial concentration and chambers' volume. Here, the relative diffusion ratio of each component was calculated as

the ratio of the measured concentration in the Blank chamber over the calculated theoretical concentration at the ideal diffusion equilibrium condition.

Bioinspired CRISPR-MCR biosensor fabrication and operation.

As shown in Supplementary Figure S1 and S2, the bioinspired CRISPR-MCR biosensor consists of two 3D-printed microfluidic parts: i) a top part and ii) a bottom part. These two parts were first designed by Solidworks software and printed by a Form 2 3D printer from FormLabs (MA, USA). Next, PES membrane obtained from Sterlitech (WA, USA) was fixed between the two parts by using ring-shaped double-sided tape. To enable waterproof sealing, 3D-printing clear resin was added between the two 3D-printed parts and treated under UV light for polymerization. Then, 150 μL water blister and personal glucose meter strip were mounted in the biosensor by using double-sided tape and epoxy AB glue, respectively. After adding the sucrose solution in the cotton, it was inserted into the catalytic chamber of the biosensor and lyophilized by the FreeZone 2.5-L benchtop freeze dry system (Labconco Corporation, MO, USA). Last, the biosensor was sealed with Microseal 'B' PCR Plate Sealing Film (Bio-Rad, CA, USA).

When the biosensor was tested, 50 μL RPA or RT-RPA reaction solution with or without target template was inserted into the RPA reaction chamber, and 50 μL CRISPR reaction solution was introduced into the CRISPR chamber. Next, the biosensor was incubated on a Mini Block Heater (VWR) for 60 min at 40°C. After incubation, one cylinder neodymium magnet with an 8 mm diameter was placed at the bottom of the RT-RPA chamber of the CRISPR-MCR biosensor. Then, the water blister was pressed down and the CRISPR reaction solution was pushed into the catalytic chamber along with the water in the blister. After catalytic incubation at 40°C, the electrochemical signal in the catalytic chamber was digitally detected and read out by a personal glucose meter. The workflow of the bioinspired CRISPR-MCR biosensor is shown in Supplementary Figure S8.

SEM, TEM morphology characterization and EDS analysis.

The SEM characterization and EDS analysis were conducted on a Nova NanoSEM 450 microscope with an electric beam operated at 2 kV and 2.0 spot. For the MB-ssDNA-invertase, the samples were washed by the buffer at least three times before SEM image acquisition. To observe cross-section images, the porous membranes were placed in liquid nitrogen for 5 min before breaking them with two tweezers. All samples were sputter coated with gold on their surface before SEM observations, but no coating was applied for the EDS analysis. The TEM characterization was conducted by FEI Tecnai 12 G2 Spirit BioTWIN with AMT NanoSprint12 camera. Before TEM image acquisition, the samples were washed by water at least three times.

Digital PCR quantification for target template.

QuantStudio™ 3D Digital PCR Master Mix v2 (Cat. #A26358) and BioRad™ Reliance One-Step Multiplex RT-qPCR Supermix (Cat. #12010176) were purchased from ThermoFisher Scientific and BioRad, respectively. According to the protocol, the PCR or RT-PCR mixture was first prepared. After 14.5 μL of reaction mixture was loaded into the 3D Digital PCR chip (Cat. # A26316) by using a 3D Digital PCR Chip Loader (Cat. # A29154), the chip was

placed on a ProFlex™ 2 x Flat Block Thermal Cycler (Cat. # A26316) for PCR reaction. At the end of the PCR/RT-PCR reaction, the chip was read on either QuantStudio™ 3D Digital PCR Instrument (Cat. # A26316) or a fluorescence microscope Axio Observer from ZEISS.

Clinical sample preparation and RT-PCR detection.

All clinical plasma samples were de-identified and in compliance with ethical regulations and under the approval of the Institutional Review Board of the University of Connecticut Health Center (protocol #: 21–014-2). HIV RNA samples were extracted from clinical samples using the QIAamp Viral RNA Mini Kit from QIAGEN (Hilden, Germany) according to the manufacturer's protocol. A real-time fluorescence RT-PCR assay was used to detect HIV RNA. The GoTaq Probe 1-Step RT-qPCR kit from Promega (WI, USA) was used to prepare the RT-PCR reaction solution. The 20 μL RT-PCR mix included 1× GoTaq Probe Master Mix, 1× GoScript RT Mix for 1-Step RT-qPCR, 0.5 μM HIV forward primer, 0.5 μM HIV reverse primer, 0.2 probe, and 2 μL of the target. The RT-PCR protocol contains three steps: i) reverse transcription (15 min at 45°C), ii) RT inactivation and polymerase activation (2 min at 95°C), and iii) denaturation and extension (40 cycles of 15 s at 95°C and 60 s at 60 °C). Real-time fluorescence PCR/RT-PCR detection was performed using the Bio-Rad CFX96 Touch Real-Time PCR Detection System.

Statistical analysis.

Statistical significance analyses were performed by OriginLab 2020. All statistical analyses were performed using a one-way analysis of variance (ANOVA), where n. s. = not significant with $p > 0.05$, and the asterisks (*, **, ***, ****) denote significant differences with p values (* = $0.001 < P \leq 0.05$, ** = $0.0001 < P \leq 0.001$, *** = $0.00001 < P \leq 0.0001$, **** = $P \leq 0.00001$).

Supplementary Material

Refer to Web version on PubMed Central for supplementary material.

ACKNOWLEDGEMENTS

The work was supported, in part, by the National Institutes of Health, United States, R61 AI154642 and R01 EB023607.

REFERENCES

(1). Barré-Sinoussi F; Chermann JC; Rey F; Nugeyre MT; Chamaret S; Gruest J; Dauguet C; Axler-Blin C; Vézinet-Brun F; Rouzioux C; Rozenbaum W; Montagnier L Isolation of a T-Lymphotropic Retrovirus from a Patient at Risk for Acquired Immune Deficiency Syndrome (AIDS). Science (80-.). 1983, 220 (4599), 868–871.

(2). Manoto SL; Lugongolo M; Govender U; Mthunzi-Kufa P Point of Care Diagnostics for HIV in Resource Limited Settings: An Overview. Med. 2018, 54 (1), 1–14.

(3). K. DP; Jienchi D; Andrew B; Lorraine L; Francesco M; Jilian S; Anna B; S. BD; D. PJ; Nigel G Point-of-Care HIV Viral Load Testing: An Essential Tool for a Sustainable Global HIV/AIDS Response. Clin. Microbiol. Rev 2019, 32 (3), e00097–18. [PubMed: 31092508]

(4). Gootenberg JS; Abudayyeh OO; Lee JW; Essletzbichler P; Dy AJ; Joung J; Verdine V; Donghia N; Daringer NM; Freije CA; Myhrvold C; Bhattacharyya RP; Livny J; Regev A; Koonin EV; Hung

DT; Sabeti PC; Collins JJ; Zhang F Nucleic Acid Detection with CRISPR-Cas13a/C2c2. Science (80-.). 2017, 356 (6336), 438–442.

(5). Gootenberg JS; Abudayyeh OO; Kellner MJ; Joung J; Collins JJ; Zhang F Multiplexed and Portable Nucleic Acid Detection Platform with Cas13, Cas12a, and Csm6. Science (80-.). 2018, 360 (6387), 439–444.

(6). Chen JS; Ma E; Harrington LB; Da Costa M; Tian X; Palefsky JM; Doudna JA CRISPR-Cas12a Target Binding Unleashes Indiscriminate Single-Stranded DNase Activity. Science (80-.). 2018, 360 (6387), 436–439.

(7). Broughton JP; Deng X; Yu G; Fasching CL; Servellita V; Singh J; Miao X; Streithorst JA; Granados A; Sotomayor-Gonzalez A; Zorn K; Gopez A; Hsu E; Gu W; Miller S; Pan CY; Guevara H; Wadford DA; Chen JS; Chiu CY CRISPR–Cas12-Based Detection of SARS-CoV-2. Nat. Biotechnol 2020, 38 (7), 870–874. [PubMed: 32300245]

(8). Ganbaatar U; Liu C CRISPR-Based COVID-19 Testing: Toward Next-Generation Point-of-Care Diagnostics. Frontiers in Cellular and Infection Microbiology. 2021, 11, 663949. [PubMed: 33996635]

(9). Deng J; Zhao S; Liu Y; Liu C; Sun J Nanosensors for Diagnosis of Infectious Diseases. ACS Appl. Bio Mater 2021, 4 (5), 3863–3879.

(10). Wang H; Zhao Z; Liu Y; Shao C; Bian F; Zhao Y Biomimetic Enzyme Cascade Reaction System in Microfluidic Electrospray Microcapsules. Sci. Adv 2022, 4 (6), eaat2816.

(11). Szostak JW; Bartel DP; Luisi PL Synthesizing Life. Nature 2001, 409 (6818), 387–390. [PubMed: 11201752]

(12). Cancino J; Capalbo A; Di Campli A; Giannotta M; Rizzo R; Jung JE; Di Martino R; Persico M; Heinklein P; Sallese M; Luini A Control systems of membrane transport at the interface between the endoplasmic reticulum and the Golgi. Developmental Cell. 2014, 30(3), 280–94. [PubMed: 25117681]

(13). Pigeolet E; Corbisier P; Houbion A; Lambert D; Michiels C; Raes M; Zachary M-D; Remacle J Glutathione Peroxidase, Superoxide Dismutase, and Catalase Inactivation by Peroxides and Oxygen Derived Free Radicals. Mech. Ageing Dev 1990, 51 (3), 283–297. [PubMed: 2308398]

(14). Kuk SK; Singh RK; Nam DH; Singh R; Lee JK; Park CB Photoelectrochemical Reduction of Carbon Dioxide to Methanol through a Highly Efficient Enzyme Cascade. Angew. Chemie - Int. Ed 2017, 56 (14), 3827–3832.

(15). Park JO; Rubin SA; Xu Y-F; Amador-Noguez D; Fan J; Shlomi T; Rabinowitz JD Metabolite Concentrations, Fluxes and Free Energies Imply Efficient Enzyme Usage. Nat. Chem. Biol 2016, 12 (7), 482–489. [PubMed: 27159581]

(16). Liu Y; Du J; Yan M; Lau MY; Hu J; Han H; Yang OO; Liang S; Wei W; Wang H; Li J; Zhu X; Shi L; Chen W; Ji C; Lu Y Biomimetic Enzyme Nanocomplexes and Their Use as Antidotes and Preventive Measures for Alcohol Intoxication. Nat. Nanotechnol 2013, 8 (3), 187–192. [PubMed: 23416793]

(17). Zhang Y; Baekgaard-Laursen M; Städler B Small Subcompartmentalized Microreactors as Support for Hepatocytes. Adv. Healthc. Mater 2017, 6 (15).

(18). Yin K; Ding X; Li Z; Zhao H; Cooper K; Liu C Dynamic Aqueous Multiphase Reaction System for One-Pot CRISPR-Cas12a-Based Ultrasensitive and Quantitative Molecular Diagnosis. Anal. Chem 2020, 92 (12), 8561–8568. [PubMed: 32390420]

(19). Wang R; Qian C; Pang Y; Li M; Yang Y; Ma H; Zhao M; Qian F; Yu H; Liu Z; Ni T; Zheng Y; Wang Y OpvCRISPR: One-Pot Visual RT-LAMP-CRISPR Platform for SARS-Cov-2 Detection. Biosens. Bioelectron 2021, 172, 112766. [PubMed: 33126177]

(20). Pang B; Xu J; Liu Y; Peng H; Feng W; Cao Y; Wu J; Xiao H; Pabbaraju K; Tipples G; Joyce MA; Saffran HA; Tyrrell DL; Zhang H; Le XC Isothermal Amplification and Ambient Visualization in a Single Tube for the Detection of SARS-CoV-2 Using Loop-Mediated Amplification and CRISPR Technology. Anal. Chem 2020, 92 (24), 16204–16212. [PubMed: 33238709]

(21). Spoelstra WK; Jacques JM; Gonzalez-Linares R; Nobrega FL; Haagsma AC; Dogterom M; Meijer DH; Idema T; Brouns SJJ; Reese L CRISPR-Based DNA and RNA Detection with Liquid-Liquid Phase Separation. Biophys. J 2021, 120 (7), 1198–1209. [PubMed: 33617832]

(22). Hu M; Qiu Z; Bi Z; Tian T; Jiang Y; Zhou X Photocontrolled CrRNA Activation Enables Robust CRISPR-Cas12a Diagnostics. Proc. Natl. Acad. Sci 2022, 119 (26), e2202034119. [PubMed: 35727982]

(23). Ding X; Yin K; Li Z; Lalla RV; Ballesteros E; Sfeir MM; Liu C Ultrasensitive and Visual Detection of SARS-CoV-2 Using All-in-One Dual CRISPR-Cas12a Assay. Nat. Commun 2020, 11 (1), 1–10. [PubMed: 31911652]

(24). Orooji Y; Faghih M; Razmjou A; Hou J; Moazzam P; Emami N; Aghababaie M; Nourisfa F; Chen V; Jin W Nanostructured Mesoporous Carbon Polyethersulfone Composite Ultrafiltration Membrane with Significantly Low Protein Adsorption and Bacterial Adhesion. Carbon N. Y 2017, 111, 689–704.

(25). Arkhangelsky E; Kuzmenko D; Gitis V Impact of Chemical Cleaning on Properties and Functioning of Polyethersulfone Membranes. J. Memb. Sci 2007, 305 (1), 176–184.

(26). Ding X; Li Z; Liu C Monolithic, 3D-Printed Lab-on-Disc Platform for Multiplexed Molecular Detection of SARS-CoV-2. Sensors Actuators B Chem. 2022, 351 (August 2021), 130998.

(27). Yin K; Ding X; Xu Z; Li Z; Wang X; Zhao H; Otis C; Li B; Liu C Multiplexed Colorimetric Detection of SARS-CoV-2 and Other Pathogens in Wastewater on a 3D Printed Integrated Microfluidic Chip. Sensors Actuators B Chem. 2021, 344, 130242.

(28). Li Z; Ding X; Yin K; Avery L; Ballesteros E; Liu C Instrument-Free, CRISPR-Based Diagnostics of SARS-CoV-2 Using Self-Contained Microfluidic System. Biosens. Bioelectron 2022, 199 (December 2021), 113865.

(29). Xiang Y; Lu Y Using Personal Glucose Meters and Functional DNA Sensors to Quantify a Variety of Analytical Targets. Nat. Chem 2011, 3 (9), 697–703. [PubMed: 21860458]

(30). Huang D; Shi Z; Qian J; Bi K; Fang M; Xu Z A CRISPR-Cas12a-Derived Biosensor Enabling Portable Personal Glucose Meter Readout for Quantitative Detection of SARS-CoV-2. Biotechnol. Bioeng 2021, 118 (4), 1587–1596. [PubMed: 33410130]

(31). Yao Q; Song D; Xu X Robust Finger-Vein ROI Localization Based on the 3σ Criterion Dynamic Threshold Strategy. Sensors . 2020.

(32). Chen Q; Yao C; Yang C; Liu Z; Wan S Development of an In-Situ Signal Amplified Electrochemical Assay for Detection of Listeria Monocytogenes with Label-Free Strategy. Food Chem. 2021, 358, 129894. [PubMed: 33933968]

(33). Liu C; Geva E; Mauk M; Qiu X; Abrams WR; Malamud D; Curtis K; Owen SM; Bau HH An isothermal amplification reactor with an integrated isolation membrane for point-of-care detection of infectious diseases. Analyst, 2021, 136(10), 2069–76.

(34). Nguyen LT, Smith BM, Jain PK. Enhancement of trans-cleavage activity of Cas12a with engineered crRNA enables amplified nucleic acid detection. Nature communications. 2020, 11, 1–3.

(35). Ganbaatar U; Liu C NEXT CRISPR: An enhanced CRISPR-based nucleic acid biosensing platform using extended crRNA. Sensors and Actuators B: Chemical, 2022, 369, 132296.

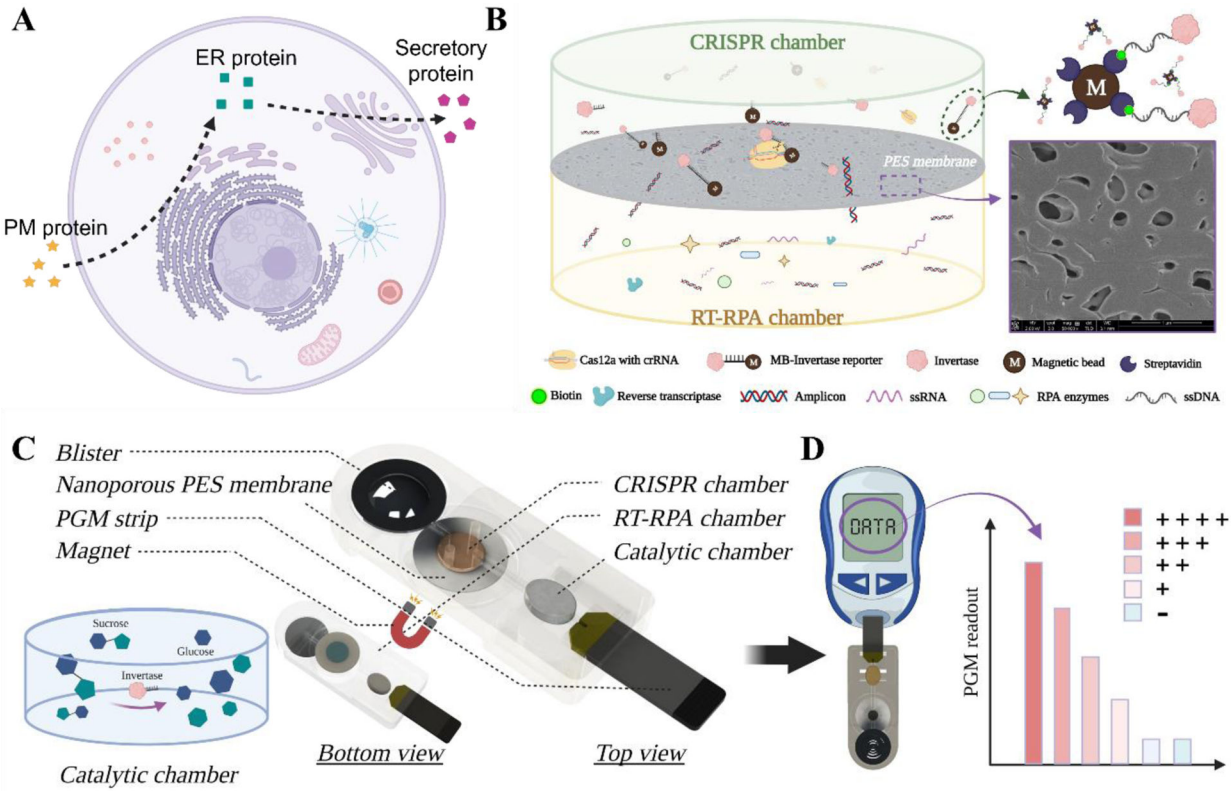

Figure 1. Bioinspired CRISPR-MCR biosensor overview.

A) Structure of a eukaryotic cell containing multi-compartment structures (e.g., subcellular organelles) for a multi-enzyme cascade reaction.[12] B) Working principle of the nanoporous membrane-separated, CRISPR-mediated cascade reaction system for HIV nucleic acid detection inspired by the eukaryotic cell. The cascade reaction system is separated by a hydrophilic nanoporous membrane (right bottom inset) into two compartments: i) an RPA or RT-RPA reaction chamber, and ii) a CRISPR reaction chamber. Due to the concentration gradient (difference), the short DNA amplicons generated by RPA exponential amplification can diffuse into the CRISPR reaction chamber through the nanoporous membrane to specifically initiate the downstream CRISPR cleavage reaction for HIV nucleic acid biosensing. C) Schematic illustration of the bioinspired CRISPR-MCR biosensor integrating the CRISPR-mediated cascade reaction system, catalytic reaction chamber, and glucose biosensing strip. Left bottom inset: catalytic chamber where pre-stored sucrose is hydrolyzed into fructose and glucose in the presence of the released invertase enzyme from the MB-ssDNA-invertase in the CRISPR reaction chamber. D) Detection of HIV nucleic acid using a personal glucose meter (PGM).

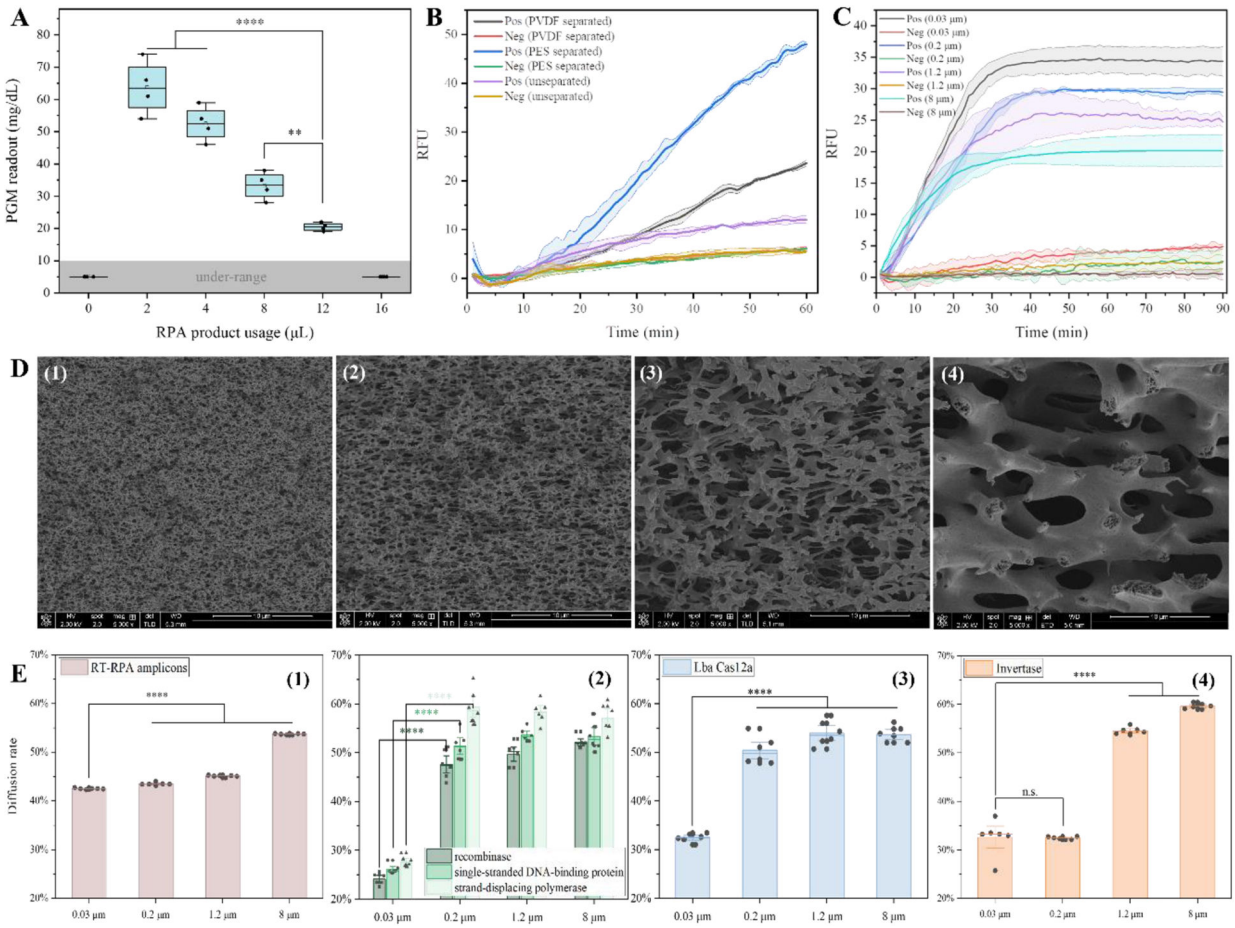

Figure 2.

Nanoporous membrane-separated, CRISPR-mediated cascade reaction system for HIV nucleic acid detection. A) Effect of the RPA reaction solution volume on the electrochemical detection of HIV nucleic acid by the glucose meter. * = 0.001 < P ≤ 0.05, ** = 0.0001 < P ≤ 0.001, *** = 0.00001 < P ≤ 0.0001. B) Comparison of real-time fluorescent detection of the RPA/CRISPR reaction with and without membrane separation. Both PES membrane and PVDF membrane were tested for comparison. C) Real-time fluorescent signal in the CRISPR-mediated cascade reaction system embedded with PES membranes of different pore sizes (0.03, 0.2, 1.2, and 8.0 μm). D) Scanning electron microscope (SEM) image of cross-sections of the PES membranes with different pore sizes (0.03, 0.2, 1.2, and 8.0 μm). E) Relative diffusion rate of different components in the CRISPR-MCR assay through the PES membranes with various pore sizes (0.03, 0.2, 1.2, and 8.0 μm). n.s., not significant with p > 0.05. The asterisks (*, **, ***, ****) denote significant differences with p values (* = 0.001 < P ≤ 0.05, ** = 0.0001 < P ≤ 0.001, *** = 0.00001 < P ≤ 0.0001, **** = P ≤ 0.00001).

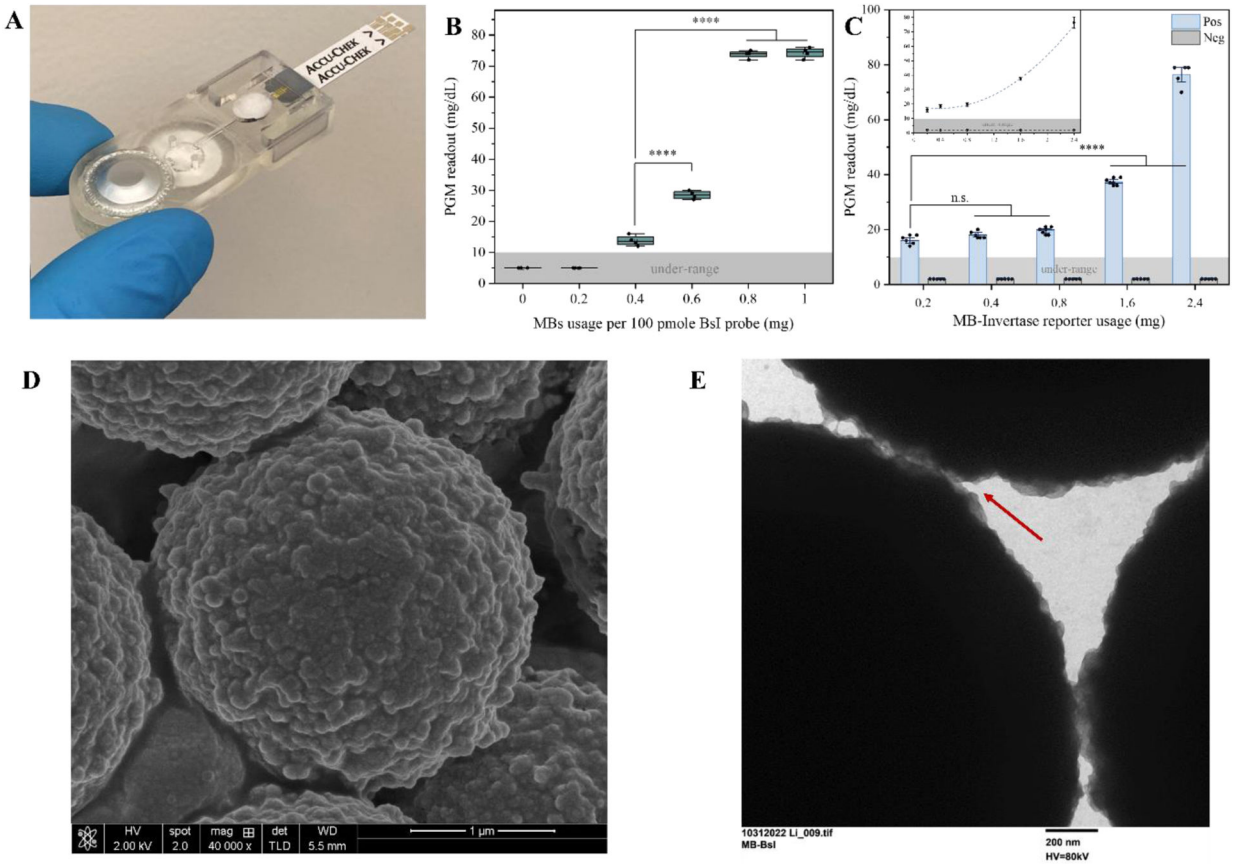

Figure 3.

Bioinspired CRISPR-MCR biosensor and its optimization. A) Photograph of the bioinspired CRISPR-MCR biosensor fabricated by 3D-printing technology. The glucose biosensing strip was incorporated into the biosensor for electrochemical detection of HIV nucleic acids by a glucose meter. B) Optimization of the usage of magnetic beads to synthesize the MB-ssDNA-invertase reporter. C) Effect of the amount of MB-ssDNA-invertase reporter on CRISPR-mediated electrochemical detection. n.s., not significant with $p > 0.05$. The asterisks (*, **, ***, ****) denote significant differences with p values (* = $0.001 < P \leq 0.05$, ** = $0.0001 < P \leq 0.001$, *** = $0.00001 < P \leq 0.0001$, **** = $P \leq 0.00001$). D) Representative SEM image of the MB-ssDNA-invertase reporter for glucose biosensing detection in the bioinspired CRISPR-MCR biosensor. E) TEM image of the MB-ssDNA-Invertase reporter.

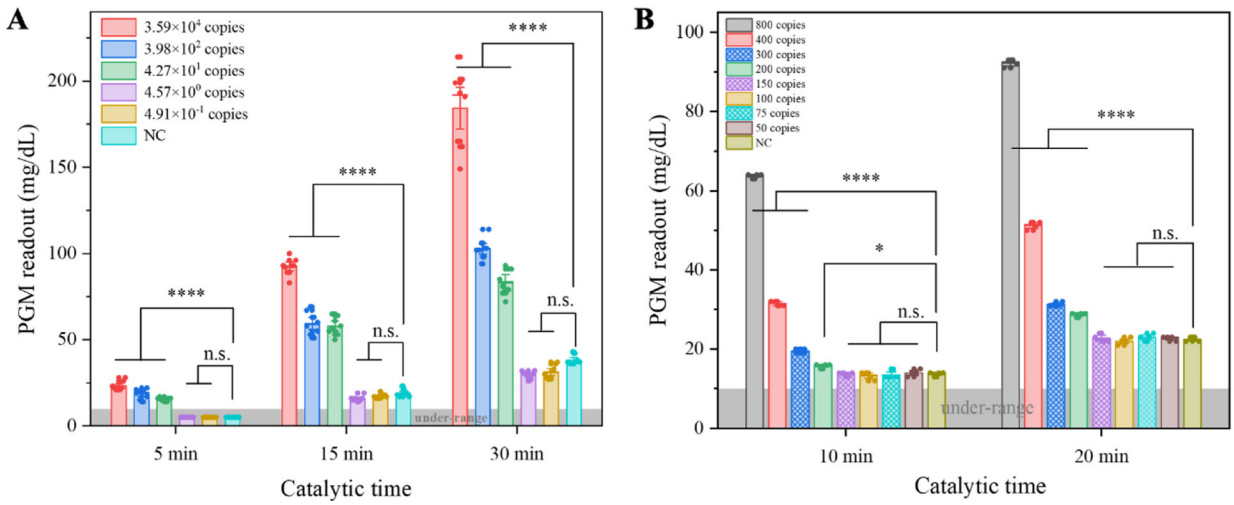

Figure 4.

Detection of HIV nucleic acids in the bioinspired CRISPR-MCR biosensor by using a glucose meter. A) HIV DNA detection in the biosensor by using a glucose meter after various catalytic reaction times of 5, 15, and 30 min. B) HIV RNA detection in the biosensor by using a glucose meter after a catalytic time of 10 and 20 min. NC, negative control. n.s., not significant with $p > 0.05$. The asterisks (*, **, ***, ****) denote significant differences with p values (* = $0.001 < P \leq 0.05$, ** = $0.0001 < P \leq 0.001$, *** = $0.00001 < P \leq 0.0001$, **** = $P \leq 0.00001$).

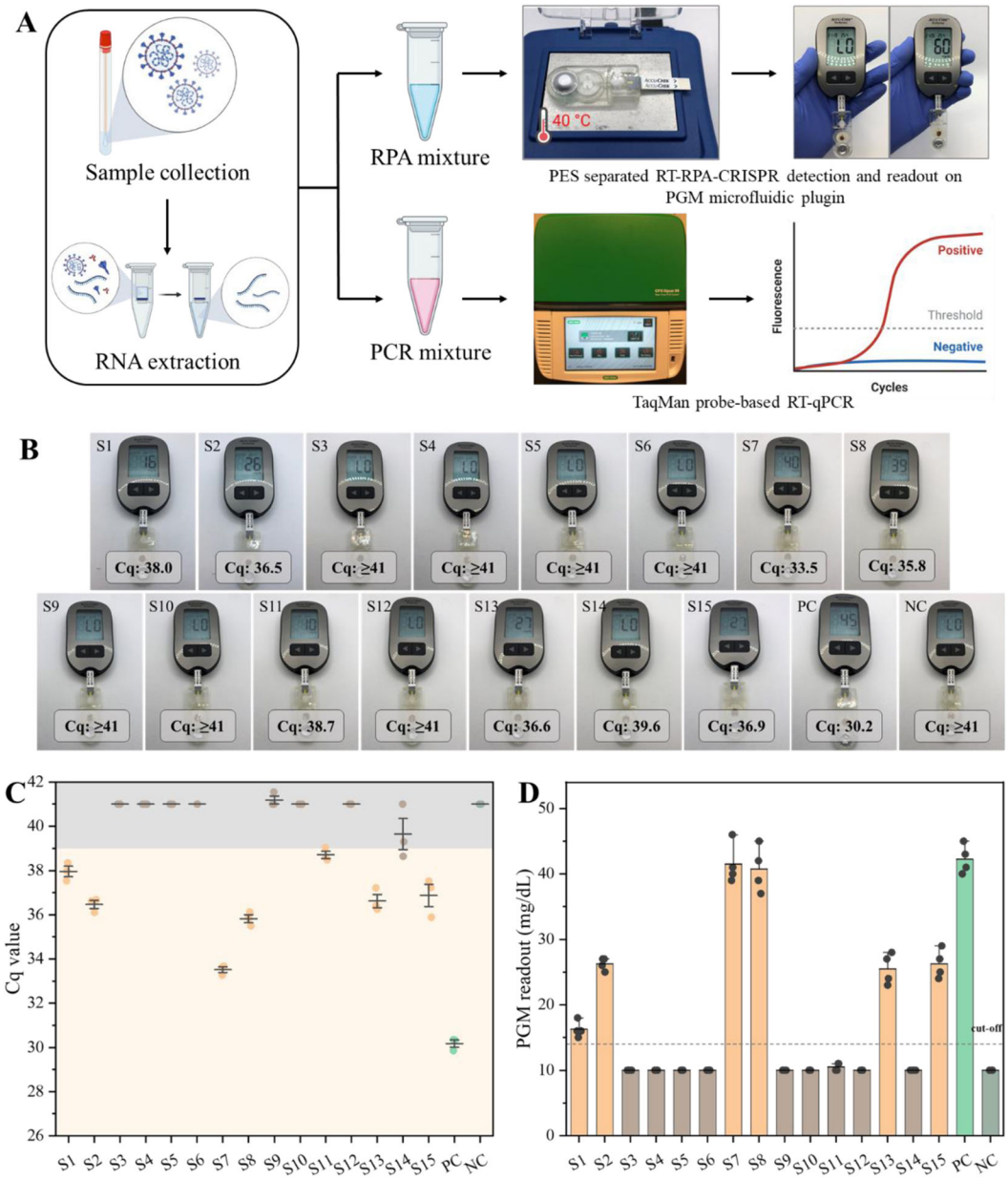

Figure 5.

Clinical validation of the bioinspired CRISPR-MCR biosensor to detect HIV virus in clinical plasma samples. A) Procedures of the CRISPR-MCR biosensor and the RT-qPCR assay for HIV detection in clinical samples. B) Representative HIV test results of 15 clinical samples and positive/negative controls by the bioinspired CRISPR-MCR biosensor. C) Cq values of the clinical plasma samples and positive/negative controls by RT-PCR. D) Detection results of HIV in clinical samples by using the CRISPR-MCR biosensor and glucose meter. PC and NC are, respectively, positive control and negative control. The cut-off threshold value was set as 14 mg/dL according to the 3σ criterion.